Filter Media Tests Under Simulated Martian Atmospheric Conditions

Juan H. Agui[1]

[1] NASA Glenn Research Center, Fluid Physics and Transport Branch, 21000 Brookpark Rd., Cleveland, OH 44135; PH (216) 433-5409; FAX (216) 433-8050; email Juan.H.Agui@nasa.gov

ABSTRACT

A human exploration program of the Martian surface will require the optimal utilization of planetary resources. One of its more abundant resources is the Martian atmosphere that can be harvested through filtration and chemical processes that purify and separate it into its gaseous and elemental constituents. Effective filtration needs to be part of the suite of resource utilization technologies. A unique testing platform has been developed at the NASA Glenn Research Center which provides the relevant operational and instrumental capabilities to test articles under the proper simulated Martian conditions. A series of tests were conducted to assess the performance of filter media. Light sheet imaging of the particle flow provided a means of detecting and quantifying particle concentrations. The media's efficiency was evaluated by gravimetric means through a two-ply filter media configuration. These tests will help to establish techniques and methods for measuring capturing efficiency and arrestance of conventional fibrous filter media for planetary surface opertions. This paper will describe initial test results on different filter media.

INTRODUCTION

The Martian atmosphere provides an accessible and versatile resource which holds great promise for sustaining surface missions. It provides an ample source of CO_2 which can be used to produce oxygen for propellants, fuel cell reactants, and life support consumable. However, one of the main challenges to harvesting resources from the Martian atmosphere are the atmospheric winds and storms that entrain and suspend dust particles, hampering atmospheric acquisition processes. Since the purification of gases rely on effective and reliable filtration systems, these systems, particularly those designed for standard terrestrial conditions, will need to be tested and demonstrated under the low pressure mostly CO_2 conditions of the Martian atmospheric.

Media filtration is a well-established and highly effective method of removing particulate matter in air and gas filtration applications, and ubiquitously used in residential, commercial and industrial settings. The filter media typically goes through rigorous and standardized methods of testing by the manufacturers and testing laboratories to certify the mechanical integrity and performance of the media for their intended application. In order to assess and gain confidence that the filter

media will perform in the Martian environment, test methods are needed that simulate relevant Martian conditions. The thin Martian atmosphere, nearly one hundredth the atmosphere on Earth, can alter the flow dynamics associated with filtration. In addition, the mostly CO_2 gaseous composition will exhibit inherently different flow properties because of the higher molecular density and lower viscosity compared to air. Although of prime importance in filter design, only limited data exists on the size of airborne particles on the Martian surface. Optical atmospheric data from the Mars Exploration Rover (MER) missions indicates particle concentrations of about 6 particles/cm^3 at a mean diameter of 3 μm (see Lemmon et al., 2004, and Landis, 2013).

Tests are under way at the NASA Glenn Research Center in a customized flow loop apparatus to assess the performance of various filter media under simulated Martian conditions. Light sheet imaging of the particle flow provides a means of detecting and quantifying particle concentrations to determine capturing efficiencies. The media's efficiency is also evaluated by gravimetric means through a two-ply filter media configuration. The tests will help to establish techniques and methods for measuring capturing efficiency and arrestance (pressure drop) of conventional fibrous filter media. This paper will describe initial test results on different grade filter media.

Filter Performance

Filter performance is predicated on the hydrodynamic response of the particle as it approaches an individual fiber in the media, known as single fiber theory. A typical fibrous filter media consists of several hundred layers of micron size fibers. Despite the high fiber density the media remains highly permeable. According to theory, each fiber can be treated in isolation with the potential for three basic capturing mechanisms: impaction, interception, and diffusion. Inertial impaction is the dominant capturing mechanism for the large diameter particle. In Figure 1, the path taken by a large diameter particle is depicted in the top streamline in which the increased inertia causes the particle to deviate from the streamline path when it encounters sufficient flow curvature. If sufficiently massive, the particle directly impacts onto the fiber surface and adheres to it. The interception mechanism is illustrated in the middle streamline as the particle comes within one radius of the surface of the fiber. In this case the particle has sufficient contact time with the fiber surface to also become trapped. Lastly, very small diameter particles, as shown in the bottom streamline, are more susceptible to Brownian motion and are intermittently and incrementally knocked off the stream path by molecular collisions. Due to the randomness of the diffusional collisions the particle has a chance to approach the fiber surface and also become trapped.

Of these mechanisms, only the impaction mechanism is affected by reduced pressures, which results from the drag reduction on the fine particle. The reduced pressure also reduces drag over the fibers in the media. Note that viscosity is nearly independent of pressure for low pressure gases, and therefore should not produce any significant changes in hydrodynamic drag. However the reduced pressure induces slip effects over small-size objects in the flow such as particles and fibers. The slip correction can be

obtained from a useful form of the Cunningham slip correction factor given by (Hinds, 1999)

$$C_c = 1 + \frac{1}{p \cdot d}\left[1.56 + 7.0e^{-.059p \cdot d}\right]$$

where p is pressure in kilopascals and d is the particle or fiber diameter in microns.

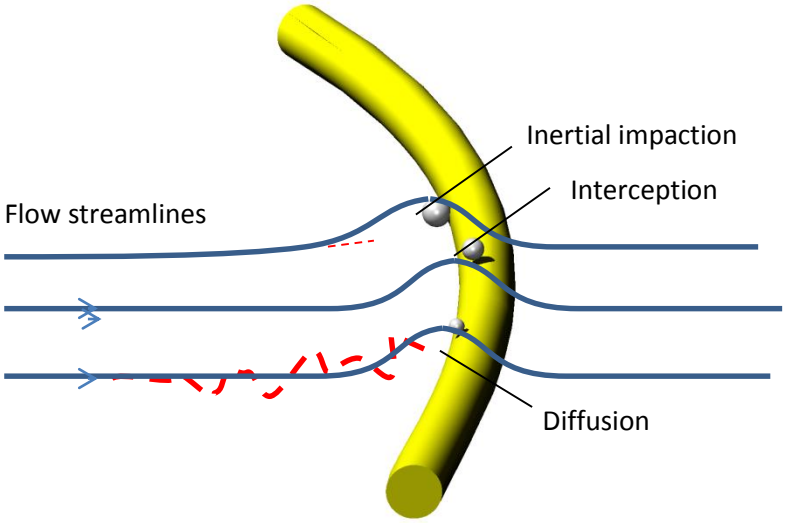

Figure 1: Particle capture on a single fiber

The consequence of particle slip is best represented on a typical filter media efficiency curve shown in Fig. 2 . The curve shows the relative importance of the different particle capture mechanisms in contributing to the shape of the efficiency curve. The diffusion regime is dominant in the range of the smallest particle diameters, sub-micron and below. A very high proportion of the particles in this size range, up to 100% at the very smallest particle sizes, get captured by the fibers throughout the media. In the upper particle size range, the super-micron range, inertial impaction and interception are the key capture mechanisms. This regime is also characterized by a very high percentage of particle capture, particularly at the largest particle sizes. In the intersecting regime between these two particle size ranges, the effect of the particle diffusion is shown to taper off while the effect of inertial impaction and interception starts to dominate. The net effect is a small reduction in filter efficiency that is characterized by a well-defined "valley" and minimum point. The concept of the Most Penetrating Particles Size (MPPS) is applicable in this range and is typically taken to be the near minimum efficiency point. The effect of particle slip is to shift the impaction regime to smaller particle diameter thus affecting the minimum efficiency and shifting the MPPS to a smaller diameter.

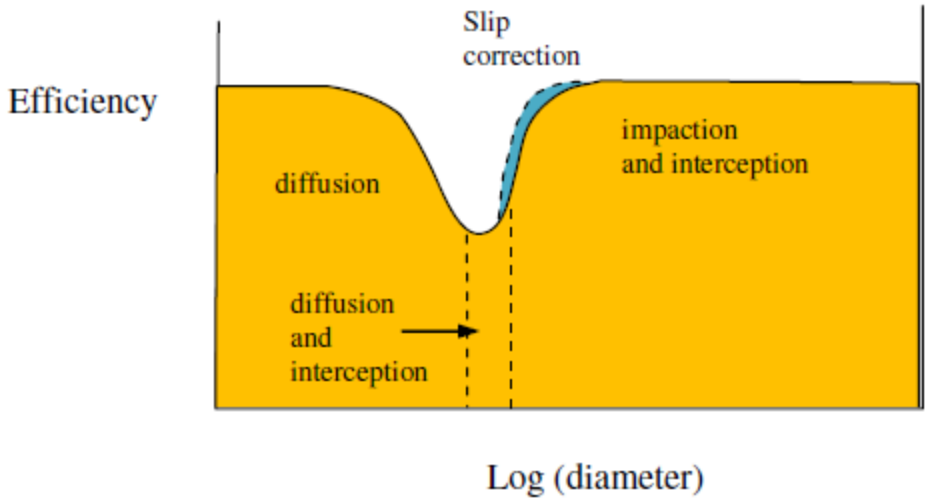

Figure 2: Filter Media Efficiency Curve.

EXPERIMENTAL SETUP

A unique testing platform at the NASA Glenn research center is being used to provide the proper testing capabilities (see Fig. 3). It consists of a sealed recirculating flow loop fabricated from 6 inch pipe segments, and contains axial fans and a vacuum pump for flow induction and low pressure operation respectively. Backfilling with alternate gases such as CO_2, which better simulates the Martian atmosphere, can be facilitated. The apparatus also has an integrated particle dispenser that internally introduces challenge particles from within the flow stream. The dispenser can hold most any type of solid granular particles, including Martian simulant fines which will be used to simulate Martian atmospheric dust. Multiple ports and viewports permit the integration of pressure and velocity sensors, light sources and imagers.

Some of the key components of the facility are shown the schematic in Fig. 4. First, a 300 l/min displacement, scroll dry (oil-free) vacuum pump (VAC) was used to achieve the Martian atmospheric pressure of 7 Torr. To introduce the CO2 gas the system is pumped down to its maximum vacuum level typically 1 Torr or less and then back filled with CO2 gas, from the supply tank, to a pressure of 7 Torr. Second, in order to ensure that clean air is returned to the test section of the flow loop, a system HEPA filter has been incorporated into the facility. DC powered axial fans (main and booster) using variable current and voltage supplies produce the axial flow. Flow straighteners for flow conditioning are placed ahead of the orifice meter. Finally, the particle generator incorporated inside the flow volume does not require any outside delivery source that could compromise the integrity of the enclosed flow. This method overcomes the challenge of incorporating standard filter efficiency test methods which introduce additional pressurized air and typically employ challenge aerosols mostly in the form of oil droplets. The particle generator internally disperses solid particles and entrains them into the facility flow upstream of the filter test

station. The device was filled with either standard calibration particles or planetary simulant dust particles prior to testing.

Since commercial optical particle counters and photometers, used in conventional filter testing, could not practically be used at vacuum pressures, a light sheet imaging technique was adapted to provide a method of recording real-time particle concentrations. A schematic of the technique is shown in Figure 5. A 527 nm pulsed Nd:YAG crystal laser generates a beam which is split, through a 50/50 beam splitter, and coupled into two optical fibers. The light emitted from the fiber is collimated and then spread into two diverging light sheets via cylindrical lenses into the flow volume. Two high speed cameras are synchronized with the laser pulses through a pulse generator distributing a TTL signal at 1 kHz to the laser and the cameras to capture images of particles crossing through the light sheets.

Two different solid challenge particles were used in these tests. The first were silica microspherical particles 0.25 μm in diameter with a 10% tolerance. These particle have been imaged under Scanning Electrical Mobility (SEM) and found to be closer to 0.27 μm in mean diameter (see Mackey et al., 2009). The use of mono-size particle of tight tolerance in this diameter range is compatible with standard techniques used in industry (e.g. ASHRAE 52.2-2007). Martian simulant similar to the JSC Mars 1 simulant was used in the second round of tests to provide more relevant exposure of dust particles on the filter sample. Allen et al. (1998) report that the simulant has a broad grain size distribution from 1 mm down to less than 5 μm. Very fine particles are known to partly make up the size fraction below 5 μm.

Figure 3: Picture of test apparatus

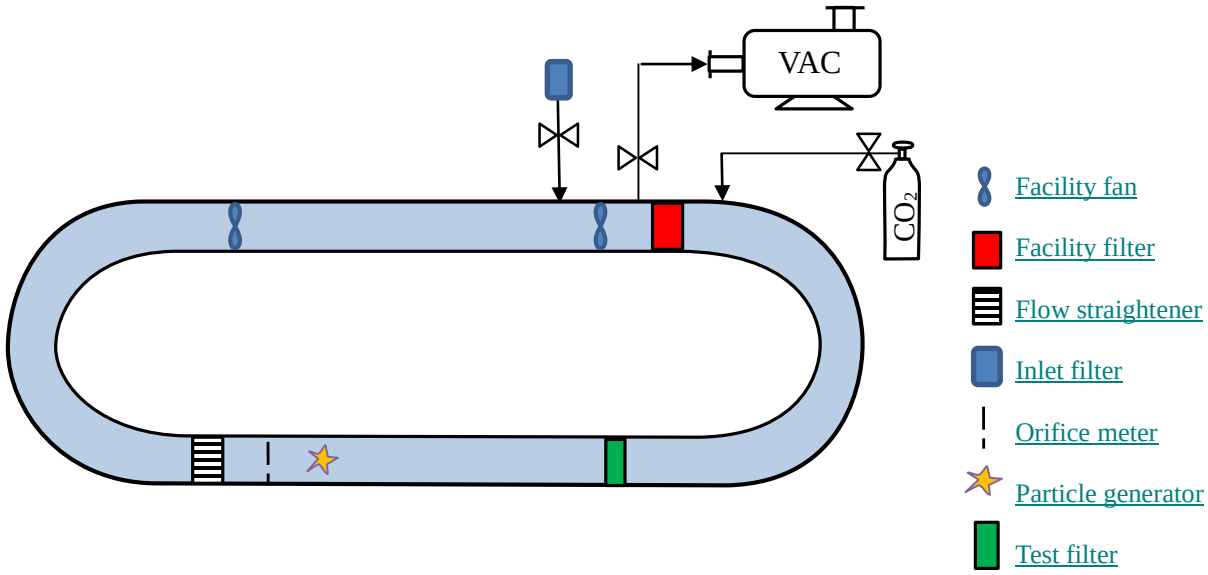

Figure 4: Schematic of flow loop apparatus

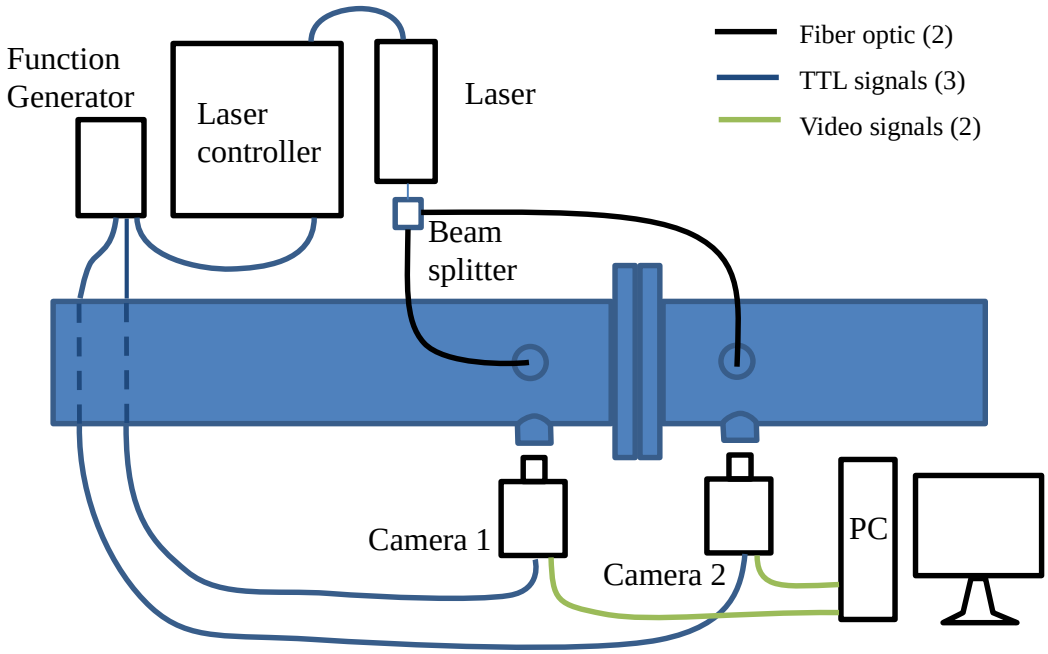

Figure 5: Imaging system setup

Various grades of filter samples were obtained from a filter manufacturer. Two different grades of filter media, a HEPA grade and a medium efficiency (60%) efficiency grade (both certified with 0.3 μm using dioctylphthalate, DOP, droplet particles), were tested. The media were cut into a circular shape and integrated into a custom filter holder that was sandwiched between pipe flanges at the test section of the flow loop.

In order to obtain a quantitative measurement of filter capturing efficiency a two-ply filter media configuration was also used. A stacked filter assembly consisting of a HEPA media, a wire mesh screen (59% open area), and a medium efficiency grade filter media was prepared for testing. The assembly was installed in the flow loop with the medium efficiency media as the first element facing the incoming particle flow. When exposed to loading of particles the lower grade media will allow a percentage of the particles in the MPPS range to penetrate through to the underlying HEPA media. This configuration permits the determination of filter performance through gravimetric measurement of the particle mass loaded on each media layer.

RESULTS

The generalized discharge coefficient equation for orifice flows was used to calculate the flow rates for each configuration.

$$Q = C_d A_t \sqrt{\frac{2\Delta p}{\rho}}$$

A value of 0.6 was used for the discharge coefficient, C_d, in all cases. This assumes that at the low Martian pressure of 7 Torr, the fluid medium is still considered a continuum. This applies for very small Knudsen numbers, $Kn << 1$, given by,

$$Kn = \frac{\lambda}{L}$$

Where λ is the mean free path of the medium and L is the characteristic length scale. At Martian pressure where $\lambda \sim 1$ μm, the Knudson number based on orifice throat diameter is estimated to be 2×10^{-5}, which is well within continuum range. Also, Raju (1994) has performed tests of rectangular slits and nozzles and shows that the C_d starts to asymptote to its standard value above a Reynolds number based on orifice throat area of 10, which is the case in these tests.

The achievable flow rates and pressure drops for each filter media sample and operating conditions are presented in Table 1.

Table 1: Test Configurations

Media	*Pressure (Torr)*	*Particles*	*Gas*	*Flow velocity (m/s)*	*Pressure drop (inch H_2O)*
Medium eff.	760	0.5 µm silica	Air	0.263	1.034
Medium eff.	7	0.5 µm silica	Air	0.11	2 0.022
Medium eff.	7	0.5 µm silica	CO_2	0.464	0.312
HEPA	760	0.25 µm silica	Air	0.076	1.307
HEPA	7	0.25 µm silica	Air	0.121	0.03
HEPA	7	0.25 µm silica	CO_2	.246	.477

The flow velocities obtained were slightly higher than the recommended face velocity of 0.05 m/s used in standard filter tests, even when the lowest fan settings were used. Flow rates and velocity were dependent on media permeability and the flow and operating conditions. The lowest velocities were obtained with the HEPA media and at 7 Torr in air, while the highest velocities were produced when operating at 7 Torr in CO_2 gas. In terms of pressure drop, the data show a clear reduction in pressure drop at Martian atmospheric pressure in both the air and CO_2 cases. Slip effect on the media fibers is the main factor that would contribute to drag reduction through the media. This implies that pumps and blowers will likely require less power when operated with media filters on Mars.

The light sheet images at the upstream and downstream stations are shown in Figure 6. These images were taken with no filter placed between the two stations, and therefore similar particle flows are expected in both. As can be seen there are some different optical or imaging characteristics between the two stations. Although care was taken to optically isolate the work volume there were still some stray light and reflections that restricted or diminished the imaging quality and resolving power. The steps taken included directly interfacing the transmitting optics and camera lenses on the viewport to minimize outside light, and taping strips of black dull material on the bottom surface where the light sheet shines to minimize internal reflections. The two cameras, which were of the same type and from the same manufacturer, were also swapped to check for image quality and sensitivity differences, but no apparent differences were found. The two images show representative particle populations in both imaging stations. A moderate and similar amount of particles can be observed in each image which indicated that the two-camera imaging system was a suitable technique for these tests.

Particle populations and concentrations obtained through image analysis provided an indication of the filter performance. Populations were obtained by running still images of the particle flow through a particle analyzing routine in the image processing software. Figure 7 shows an upstream image which has been processed to isolate and identify individual particles. The bottom image shows the result of image processing which provides a total count of detected particles. Particle concentrations were calculated by dividing the particle populations by the light sheet probe volume in the images. The light sheet actually forms a diverging ellipsoidal cylinder as it is

transmitted down the pipe cross-section. The probe volume is the portion of the light sheet that is imaged by the high speed cameras.

The upstream images obtained by challenging with the 0.25 μm silica particles (measured as 0.27 μm) show significant particle concentrations of up to 5 particles/cm^3. However, little to no traceable downstream concentrations are observed with the medium efficiency media. At ambient pressure, occasional or intermittent appearances of particles can be seen in the downstream images. However, at the 7 Torr in air or in CO2 virtually no individual particles are seen. Similar results were also found when the Martian simulant was used. This seems to indicate an enhancement of the filtration performance at low pressures. No downstream particles were observed with either the silica or Martian simulant particles when the HEPA media was tested. A word of caution is warranted regarding the lack of particles seen on the downstream side. Particle light scattering is limited below a certain size, and therefore it is likely that very fine particles are not being accounted for in either the upstream and downstream imaging locations. While the silica particles could be resolved, finer particles in the Martian simulant may not have been. This factor would have been more consequential in the downstream side where small particles are the ones more likely to be present in this location. Melling (1997) showed that the scattering cross section, a measure of the scattering intensity, of seeding particles, which depends on the wavelength of the incident light and the mass number (molecular density) of the particle, starts to diminish in the sub-micron range. This implies that very fine particles, smaller than the silica particles, may not have been detected. It is possible that higher power and smaller wavelength light can help improve the scattering cross section.

The two-ply media test was performed to obtain gravimetric analysis of filter performance. The gravimetric analysis clearly showed a measured penetration in the medium efficiency media. When subjected to Martian simulant in a CO_2 Martian atmospheric pressure flow, the medium efficiency filter produced a penetration of 56%, or 44% capturing efficiency, when subjected to the bulk of Martian simulant dust particles in the flow. Note that this technique is limiting in that multiple hours of testing on one media sample would be required in order to obtain sufficient particle mass to perform the analysis. This result is different from the rated efficiency of 60%, but not surprising because of the higher flow rates used in the test and that fact that the efficiency rating is for a MPPS of 0.3 μm. Figure 8 shows a comparison between the upstream medium efficiency media (left) and the downstream HEPA media (right). A noticeable brown/beige tint can be seen on the upstream media from the particle loading, most clearly delineated by the sharp boundary near the circumferential edge of the media. The very uniform particle covering on the media sample shows that full and uniform particle dispersion was achieved throughout the pipe cross section at the test station location. It also shows that there are a lack of large particles or particle clumps that are being transported in the particle flow. This is an indication that the particle generator was effective in breaking up particle clumps and released mostly single particles from the source.

Although the underlying HEPA grade media collected a portion of the particle mass, as evidence by the gravimetric analysis, no visible signs of particle deposition could be visually observed on the downstream HEPA media. This suggests that particles are getting through the medium efficiency media, but these particles are so fine in size that they are not visually detectable on the HEPA media. It also suggests that the Martian simulant carried by the simulated Martian flow contains a high percentage of fines, as much as about 40% by weight of the full size fraction of of the source simulant. This result is relevant to the Martian environment since the settling velocity of submicron particles is at least an order of magnitude lower than micron or super-micron size particles. The implication here is that a two-stage filtration system may be required to tackle the two size fractions of the airborne dust on Mars.

The two techniques presented here were found to be complimentary for this application, depending on filtration and particle size requirement. Requirements targeting particles of 0.25 μm and larger can be evaluated by testing with both the imaging and gravimetric techniques, while for even smaller particles and high efficiency media the gravimetric method alone may be more appropriate. Even in the latter case the use of light sheet imaging with polydisperse particles, such as the Martian simulant, provides a means of monitoring and evaluating the particle flow and concentrations ahead of the filter test article.

CONCLUSIONS

In order to assess the performance of media filters for atmospheric acquisition on the Martian surface a series of tests were performed in a simulated Martian atmospheric environment. Test methods using light sheet imaging, operations that simulate the Martian environment, and gravimetric analysis are being developed to establish methods of determining filter performance under these conditions. Light sheet imaging provided a method of determining instantaneous particle populations and concentrations, although there may be limitations in detecting very fine particles. Gravimetric analysis of a two-ply media test offers a robust method of determining filter efficiency. Future improvements to the light sheet imaging technique include optimizing the optics for increased light intensity, and measures to reduce stray and reflected light effects. A future program of additional tests for increased statistical significance and with different grade media will help increase the robustness of the test methods, and will provide a database of media test data under Martian conditions for future missions.

REFERENCES

Agui, J.H. Mackey, J. Vijayakumar, R. Seitz, T.M. and Brigg, V (2010) “Investigation of the Filtration of Lunar Dust Simulants at Low Pressures,” 40th International Conference on Environmental Systems, Barcelona, Spain.

Allen, C.C., Morris, R.V., Jager, K.M. Golden, D.C., Lindstrom, D.J., Lindstrom, M.M and Lockwood, J.P. (1998) "Martian regolith simulant JSC Mars-1." In Lunar and planetary science conference, vol. 29, p. 1690.

Landis, G (2013) Private communication, Cleveland, OH.
Lemmon, M., Wolff, M. J., Smith, M. D., Clancy, R. T., Banfield, D., Landis, G. A., Ghosh, A., Smith, P. H., Spanovich, N., Whitney, B., Whelley, P., Greeley, R., Thompson, S., Bell, J. F., and Squyres, S. W. (2004), "Atmospheric Imaging Results from the Mars Exploration Rovers: Spirit and Opportunity," Science, 306, 1753-1756.
Mackey, J. and Agui, J., "Lunar Dust Cloud Characterization in a Gravitational Settling Chamber Experiencing Zero, Lunar, Earth and 1.8-g Levels," SAE Technical Paper 2009-01-2357, 2009, doi:10.4271/2009-01-2357.
Mellling, A (1997) “Tracer particles and seeding for particle image velocimetry,” Meas. Sci. Technol. 8, 1406–1416.
Raju, C. and J. Kurian, J. (1994) "Experimental investigation of rarefied gas flow through rectangular slits and nozzles" by in Experiments in Fluids, 1994, vol. 17, issue 4, pp 220-224.

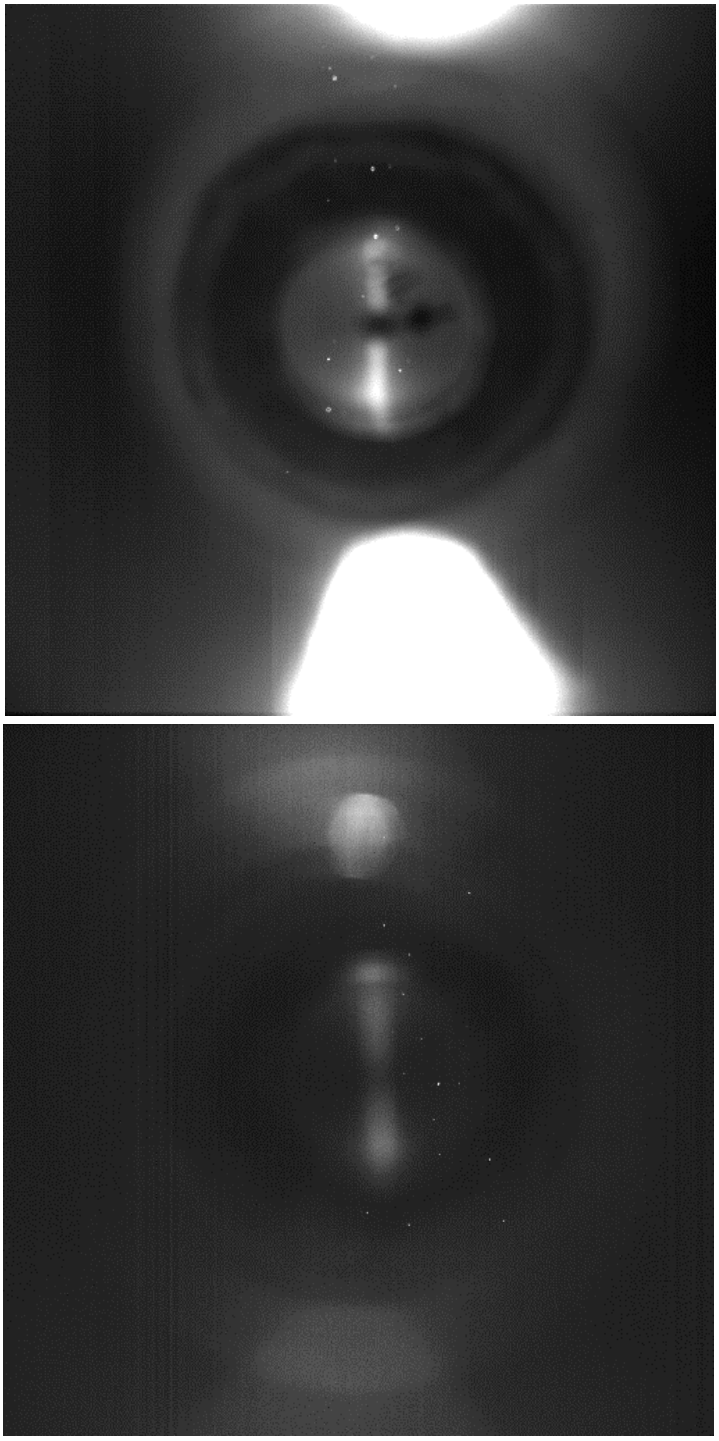

Figure 6: Comparison of upstream and downstream images

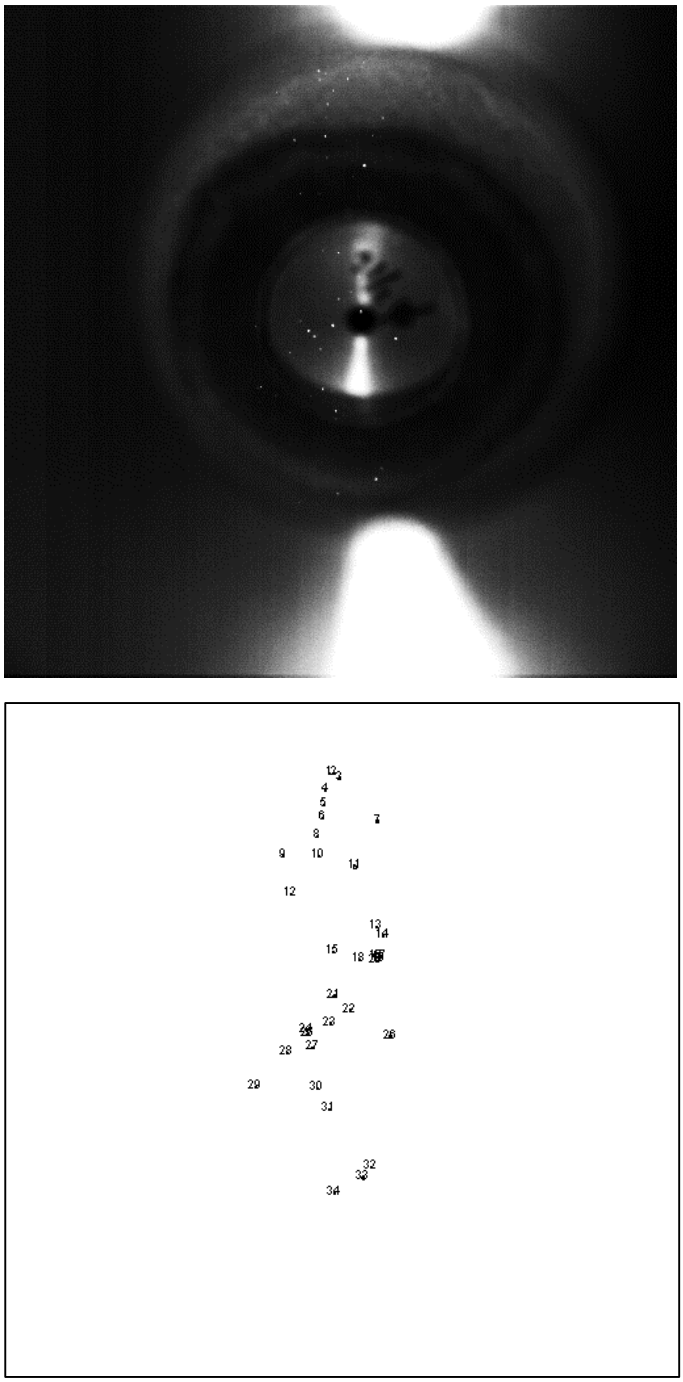

Figure 7: (a) Images of upstream particle populations and (b) processed image

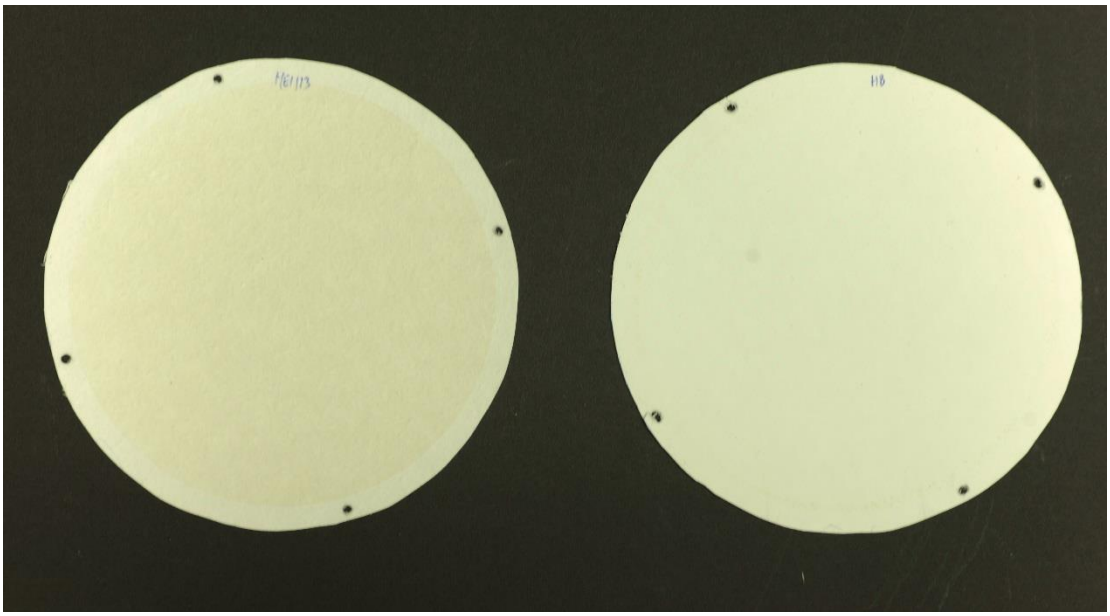

Figure 8: Side by side comparison of two-ply media test: upstream media sample (left) and downstream media sample (right).